INSTITUTE OF PHYSICS PUBLISHING JOURNAL OF PHYSICS D: APPLIED PHYSICS

J. Phys. D: Appl. Phys. **39** (2006) 2079–2083 doi:10.1088/0022-3727/39/10/016

Photoluminescent spectroscopy measurements in nanocrystalline praseodymium doped zirconia powders

F Ramos-Brito[1,5], H Murrieta S[2], J Hernández A[2], E Camarillo[2], M García-Hipólito[3], R Martínez-Martínez[3], O Álvarez-Fragoso[3] and C Falcony[4].

[1] Facultad de Ciencias Físico Matemáticas, UAdeC, A.P. 60-C, Camporredondo 25280 Saltillo Coahuila, México
[2] Instituto de Física UNAM, A.P. 20-364 Del. A. Obregón 01000 DF, México
[3] Instituto de Investigaciones en Materiales, UNAM, A.P. 70-360 Coyoacán 04510 DF, México
[4] Departamento de Física, CINVESTAV-IPN, A.P. 14-740 G.A. Madero 07000 DF, México

E-mail: framos@mate.uadec.mx and fro_brito@yahoo.com.mx

Received 13 December 2005
Published 5 May 2006
Online at stacks.iop.org/JPhysD/39/2079

Abstract

Praseodymium doped zirconia powder (ZrO_2: (0.53 at%) Pr^{3+}) was prepared by a co-precipitation technique and annealed in air at a temperature $T_a = 950\,^{\circ}C$. The x-ray diffraction pattern shows a nanocrystalline structure composed of 29.6% monoclinic and 70.4% cubic-tetragonal phases. Medium infrared and Raman analysis confirms the monoclinic/cubic-tetragonal crystalline structure and proves the absence of praseodymium aggregates in the material. Photoluminescent spectroscopy over excitations of 457.9 and 514.9 nm (at 20 K), shows two emission spectra composed of many narrow peaks in the visible–near infrared region (VIS-NIR) of the electromagnetic spectrum, associated with 4f inter-level electronic transitions in praseodymium ions incorporated in the zirconia. Excitation and emission spectra show the different mechanisms of the direct and non-direct excitation of the dopant ion (Pr^{3+}), and the preferential relaxation of the material by charge transfer from the host (zirconia) to the 4f5d band and the 4f inter-level of the dopant ion (Pr^{3+}). No evidence of energy transfer from the host to the dopant was observed.

1. Introduction

Due to its high refractive index, wide energy band gap, low optical loss, chemical and photochemical stability and excellent mechanical, electrical, thermal, and optical properties [1], zirconium oxide has been used widely as an interferometry filter and high power laser mirror [2]. On the other hand, the low phonon energy of ZrO_2 decreases the probability of non-radiative multiphonon relaxation of excited rare-earth dopant ions throughout the vibrational bands of the host. This decay process is considered one of the most competitive non-radiative relaxation processes for dopant ions in a luminescent material.

The growing interest in ZrO_2 in the luminescent area arises partially from the potential usefulness of zirconia crystal as a laser host [3]. However, most studies in praseodymium-doped materials have been done with a major focus on the laser area due to the possible applications in chemical, biological and medical fields, and new data storage and display techniques.

Actually rare-earth ions have been considered the most important optical activators for luminescent devices [4]. The constant interest in developing luminescent materials with higher radiative efficiency, and providing the three basic colours needed in a full colour device, has led to the synthesis

[5] Author to whom any correspondence should be addressed.

and study of rare-earth doped materials where the host materials used have a high energy band gap, low phonon energy and chemical stability over photon and electron radiations.

Studies on the optical properties and luminescence of zirconia [5, 6] and doped zirconia (Pr^{3+}, Er^{3+}, Eu^{3+}, Tb^{3+} and Sm^{3+}) have been reported previously [7–12]. This paper reports on the crystalline structure of 0.53 at% praseodymium-doped zirconia powder based on results obtained from three different characterization techniques, XRD, IR, and Raman. It shows the photoluminescent mechanisms that are involved in the photo-excitation and relaxation of praseodymium-doped zirconia powder prepared by a co-precipitation process.

2. Experimental procedure

Praseodymium-doped zirconia powders of different concentrations were prepared by a co-precipitation technique and annealing at 950 °C. The precursor powder material and the solvent were zirconium oxichloride ($ZrOC_{l2} + 8H_2O$, Aldrich Co.) and ethyl alcohol, respectively. Doping with Pr^{3+} was achieved by adding $PrCl_3 + 6H_2O$ to the precursor mixture in the range from 1 to 10 at% in relation to the Zr content in this mixture. Particle size and qualitative shape measurements were performed by scanning electron microscopy (SEM), and chemical composition characterization using energy dispersive spectroscopy (EDS), both with a Leica Cambridge Stereoscan 440 electron microscope equipped with a beryllium window x-ray detector. The crystalline structure and phase composition were analysed by x-ray diffraction (XRD), using a Siemens D-5000 with Cu Kα radiation at 1.5426 Å; Raman and infrared spectroscopy (IR) studies were carried out using a Nicolet Almega dispersive Raman spectrometer (with laser excitation centred at 532 nm and power 150 mW) and a Nicolet 750 FTIR spectrophotometer, respectively. Room and low temperature (20 K) photoluminescence excitation spectra were recorded using a conventional setup. A deuterium lamp was used and the excitation wavelength was selected using a monochromator (Acton Research) with a resolution of 1 nm; an appropriate filter rejected the undesired lines. The sample was placed in a mobile holder for aligning purposes and the emission was collected perpendicular to the pumping signal. Another Acton Research monochromator was used to scan the emission spectrum and measured using a photomultiplier tube connected to a PC. The 20 K and room temperature emission spectra were obtained with the same setup, except that the deuterium lamp used as the excitation source was replaced by the 457.9 and 514.9 nm argon laser lines.

3. Results and discussion

Different powders series were obtained by varying two parameters of the co-precipitation technique: the doping concentration and temperature annealing rate. The results show a major photoluminescence emission coming from the solution with 1 at% of $PrCl_3 + 6H_2O$, independent of the annealing rate employed. All the series of samples obtained, for different annealing rates, showed a decrease in the intensity of the luminescent emission as the $PrCl_3$ concentration increased, which was associated with the aggregation of doping activators at high concentrations that may change some

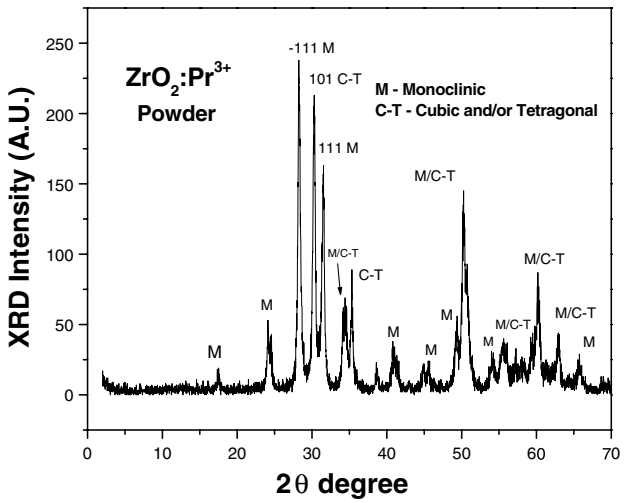

Figure 1. XRD pattern of Pr^{3+} doped zirconia powder (Zr 40.49 at%, O 58.98 at%, Pr 0.53 at%). All peaks in the pattern were associated with planes of zirconia's structural phases.

activators to quenchers and induce a related concentration quenching effect [13]. For all the powders, the one which had the greatest emission intensity was sinterized using a annealing rate of 30 °C min^{-1}, starting at T_{room} and ending at 950 °C with three stops of 20 min at 120 °C, 300 °C and 450 °C, and then keeping the sample at 950 °C for 120 min. The material resulted in a powder with a chemical composition of: Zr 40.49 at%, O 58.98 at%, Pr 0.53 at%, measured by EDS. A chemical analysis of different zones of the powder, which were selected in a random way, shows a homogeneous chemical composition over all the powder particles. All the results presented in this work refer to this powder. SEM measurements show that the powder has a very broad particle size distribution, with particles that show a flake shape with sharp edges and a flat surface, although the largest particles shown an aggregation of material on the surface, losing the flaky appearance. The morphology and the wide variety of particle sizes (between 10 and 100 μm, $\approx$30 μm being the most common size) was due to the grinding process. Analysis of the XRD measurements (figure 1) shows a polycrystalline powder structure composed of 29.6% monoclinic/70.4% cubic-tetragonal phases. The percentage of the of cubic-tetragonal phase was observed (although it is not shown in this paper) to be related to the atomic percentage of praseodymium in the material. This means that an increase in praseodymium concentration induces an increase in the cubic-tetragonal phase; this opens the possibility of obtaining a praseodymium stabilized cubic zirconia. For the type of sample studied in this work, an average crystalline grain size of 42 nm for the monoclinic phase and 48 nm for the cubic-tetragonal phase was calculated using the Scherrer's formula on the peaks centred at 2θ values of 17.52°, 24.12°, 24.52°, and 28.26° for the monoclinic phase and 30.30° and 35.50° for the cubic-tetragonal phase. The Raman spectrum obtained, but not shown for the sake of brevity, has peaks just in the 350–650 cm^{-1} region out of the entire 140–1500 cm^{-1} region and all of them are associated with vibration modes of monoclinic/cubic-tetragonal zirconia [14–16]. Figure 2 shows the IR spectra for praseodymium doped zirconia and

praseodymium oxide powders. Praseodymium oxide with a chemical composition of O 58.02 at%, Pr 22.44 at%, Cl 19.54 at% as measured by EDS, was obtained by the same procedure as for praseodymium doped zirconia. All the peaks present in the IR spectrum for praseodymium doped zirconia were assigned to the vibration modes of zirconia in its different phases [14–16], except for two of them, centred at 1389 and 1490 cm^{-1}, which were associated with the incorporation of Pr^{3+} ions in the structure of ZrO_2, since these frequencies do not appear in the IR spectrum of praseodymium oxide powder. The Raman and IR results are in agreement with the XRD results, and they do not show any new vibration frequency that could indicate the presence of praseodymium clusters, which is in agreement with the idea of the stabilization of the cubic-tetragonal phase due to the incorporation of Pr^{3+} in ZrO_2.

Figure 3 shows the 20 K emission spectrum from Pr^{3+} ion doped zirconia for the 457.9 nm excitation wavelength. There are four main peak groups, considering the emission intensity, in this spectrum. All the peaks present in the spectrum were attributed to inter-level transitions in Pr^{3+} ions incorporated in the crystalline structure of zirconia. The first group, associated with the $^3P_0 \rightarrow {}^3H_4$ Pr^{3+} transition in the region 480–530 nm, presents a multiple peak emission at 480.50, 484.75, 488.00, 493.25, 496.50, 500.75, 503.50, 506.00 and 514.25 nm, that makes the Stark splitting of the $^{2S+1}L_{2J+1}$ multiplets evident. The line at 488.00 nm results in the maximum intensity peak. These nine peaks might be associated with the the Kramer doublets of the $^3H_4$ Stark multiplet, due to the superposition of the spectra of Pr^{3+} ions incorporated in more than one zirconia crystalline phase, monoclinic and cubic/tetragonal according to the XRD results. The other three peak groups observed correspond to the $^1D_2 \rightarrow {}^3H_4$, $^3P_0 \rightarrow {}^3H_6$ and $^3P_0 \rightarrow {}^3F_{3,4}$ transitions with maximum intensity peaks at 611.5, 664.5 and 750.5 nm, respectively. Several emission peaks present when the 457.9 nm excitation light was used do not appear when the material is excited with the 514.9 nm line; these are indicated in figure 3 with an asterisk (∗) and were associated with $^3P_1 + {}^1I_6 \rightarrow {}^3F_{3,4}$, $^3P_2 \rightarrow {}^3F_{3,4}$ and $^3P_2 \rightarrow {}^1G_4$ transitions. The room temperature and 20 K emission spectra show the same number of peaks and the same relative intensity between them for the 457.9 nm excitation wavelength, which proves there is no thermal population of the electronic states. In a previous work, the excitation spectrum in the Ultraviolet (UV) region for a 616 nm emission wavelength coming from praseodymium doped zirconia was presented [7], and the band that appeared centred at 300 nm was associated with the 4f5d of the Pr^{3+} ion. Figure 4(*a*) shows the excitation spectrum for a 611.5 nm emission wavelength ($^1D_2 \rightarrow {}^3H_4$), which presents two absorption bands in the UV region localized at 245 and 300 nm that are associated with transitions from band to band in zirconia (gap ≈5 eV) and $^3H_4 \rightarrow$ 4f5d in Pr^{3+}, respectively. The presence of the 4f5d band at 300 nm indicates the possible existence of Pr^{3+} in C_2 sites of the cubic/tetragonal zirconia [17, 18]. In Figure 4(*a*), after 425 nm appears a wide absorption band associated with deep energy levels inside the gap of zirconia due to the possible creation of crystal defects with the incorporation of Pr^{3+}. The absorption by the material is being studied with diffuse reflectance spectroscopy, and the preliminary results show

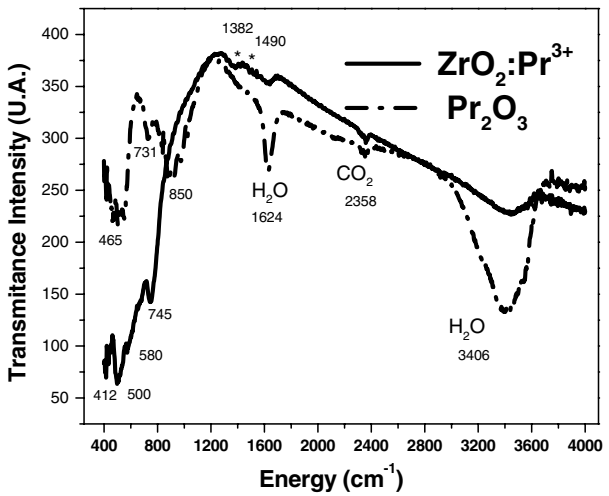

Figure 2. IRS spectrum for Pr^{3+} doped zirconia powder (Zr 40.49 at%, O 58.98 at%, Pr 0.53 at %) and praseodymium oxide (Pr 22.44 at%, O 58.02 at%, Cl 19.54 at%).

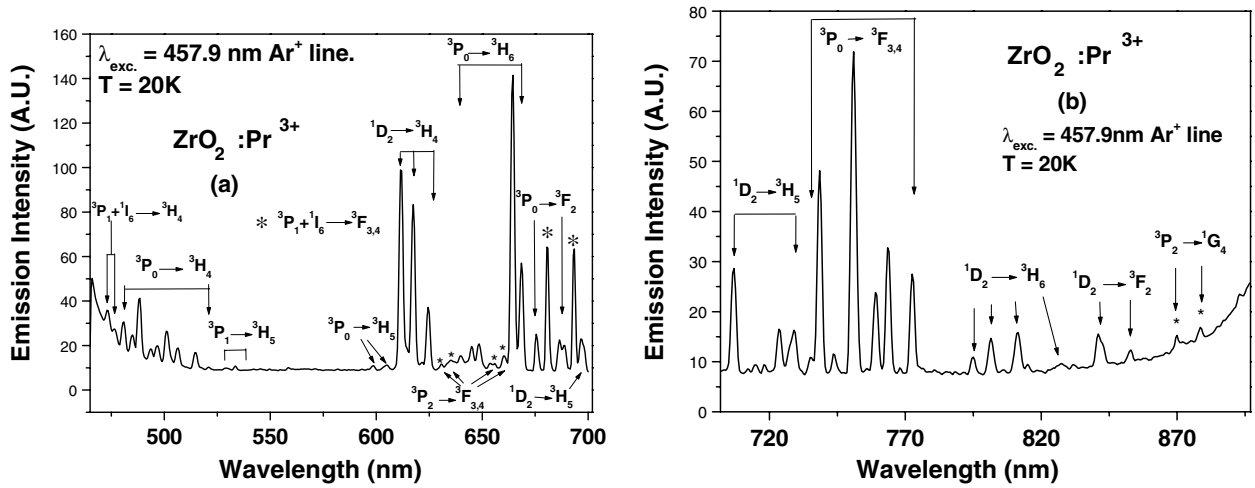

Figure 3. High resolution emission spectrum at 20 K in a 450–900 nm transition region resulting from the 457.9 nm excitation of the Pr^{3+} ions incorporated in zirconia (Zr 40.49 at%, O 58.98 at%, Pr 0.53 at%), using an argon laser. The spectrum is shown in two parts: (*a*) from 450 to 700 nm and (*b*) from 700 to 900 nm.

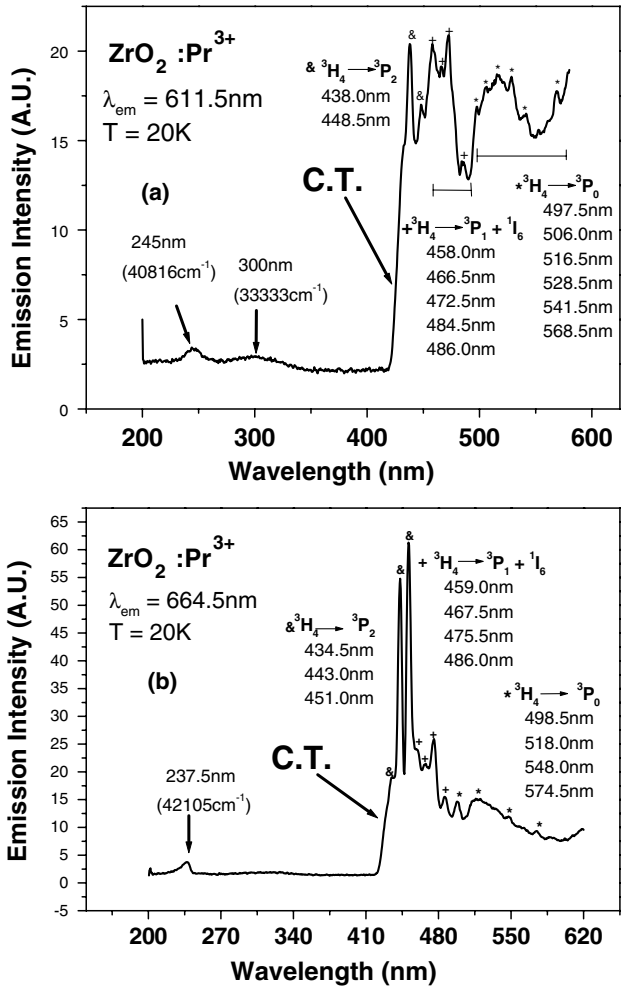

Figure 4. High resolution excitation spectrum at 20 K for Pr^{3+} doped zirconia powder (Zr 40.49 at%, O 58.98 at%, Pr 0.53 at%) for a 611.5 nm emission wavelength ($^1D_2 \rightarrow {}^3H_4$). The spectrum shows the charge transference (CT) band between deep levels of the ZrO^2 host and Pr^{3+} levels.

a wide absorption band for praseodymium doped zirconia (250–550 nm). In figure 4(*a*) praseodymium absorption peaks overlapping the end of the absorption band of the host (425–550 nm) indicate the charge transfer between the host and the dopant ion.In addition the shape of the emission spectrum in figure 3 shows the preferential relaxation of the material through the 4f5d band and the 4f inter-level of Pr^{3+}. The Pr^{3+} absorption peaks in the excitation spectrum are listed in three groups, (1) 438.0 nm and 448.5 nm, (2) 458.0, 466.5, 472.5, 484.5, and 486.0 nm, and (3) 497.5, 506.0, 516.5, 528.5, 541.5, and 568.5 nm, associated with regions of the electromagnetic spectrum corresponding to the transitions $^3H_4 \rightarrow {}^3P_2$, $^3H_4 \rightarrow {}^3P_1 + {}^1I_6$, and $^3H_4 \rightarrow {}^3P_0$. The region of the electromagnetic spectrum for $^3H_4 \rightarrow {}^3P_0$ absorption (around 500 nm) presents a band with six peaks, when it should present only one peak, associated with these being no thermal population at 20 K of the $^3H_4$ level and to these being no degeneration of the $^3P_0$ level. This result is in agreement with the incorporation of the Pr^{3+} ion in more than one spectroscopy site of the different zirconia phases present in the sample. Figure 4(*b*) shows the excitation spectrum for a 664.5 nm

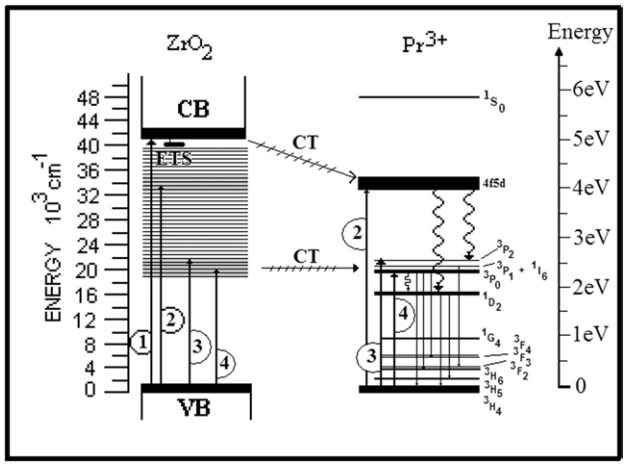

Figure 5. Energy diagram of the Pr^{3+} doped ZrO_2. The labels 1, 2, 3 and 4 represent the different excitation paths found; electronic trap states are represented by ETS. The shade band, between the valence band, VB, and the conduction band, CB, in the ZrO_2 diagram represents deep energy levels in the band gap of $ZrO_2 : Pr^{3+}$. The electronic transitions are represented by arrows and the phonon transitions by curved arrows. The CT arrows represent the charge transference between zirconia and the Pr^{3+} ion.

emission wavelength ($^3P_0 \rightarrow {}^3H_6$) which differs from the last excitation spectrum for 611.5 nm. The 443.0 and 451.0 nm absorptions corresponding to $^3H_4 \rightarrow {}^3P_2$ present a major relative intensity over the other absorptions, indicating that the most efficient path to getting an intense 664.5 nm emission is through the $^3P_2$ levels, which is even more efficient than the direct excitation of the Pr^{3+} ion into the $^3P_0$ level. This predilection could be related to two possible excitation paths for the ^3P_js in the Pr^{3+} levels: (1) charge transference from deep energy levels in the zirconia gap to ^3P_js in the Pr^{3+} levels and (2) direct excitation from the $^3H_4$ Pr^{3+} level, which probably increases the charge transference from $^3P_2$ to $^3P_0$ in the Pr^{3+} levels.

Figure 5 shows the summary results of the energy diagram of the Pr^{3+} doped ZrO_2 experimentally observed. It also describes the four excitation channels and the multiple paths of luminescent recombination sites.

4. Conclusions

We obtained ZrO_2: (0.53 at%) Pr^{3+} monoclinic/cubic-tetragonal polycrystalline powder, with an intense multiple peak photoluminescent emission, due to electronic deep states, induced in the band gap by the possible incorporation of the Pr^{3+} in C_2 cubic-tetragonal sites and others sites of the monoclinic and cubic-tetragonal crystalline phases of zirconia. The charge transfer from deep energy levels in the ZrO_2 host to ^3P_js in the Pr^{3+} levels increases the value of the capture cross section of the Pr^{3+}, increasing the luminescent efficiency process in the material. Excitations with 457.9 and 514.9 nm at 20 K showed two emission spectra composed of many narrow peaks in the visible–near infrared region of the electromagnetic spectrum, associated with the 4f inter-level electronic transitions in the praseodymium ion incorporated in different crystalline phases of zirconia. The photoluminescent excitation and emission spectra show the different mechanisms

of the direct and non-direct excitation of the activator ion (Pr^{3+}), and the preferential relaxation of the material by charge transfer from the host (zirconia) to the 4f5d band and the 4f inter-level of the activator ion (Pr^{3+}). No evidence of energy transfer from the host to the activator was observed.

Acknowledgments

The authors thank Leticia Baños, José Guzmán, J García Coronel and M Guerrero for technical support provided , OCI-UNAM (Mexico) for travel support and CoNaCyT (Mexico) for the financial grant for this investigation.

References

[1] Subbarao E C 1981 Zirconia—an overview *Science and Technology of Zirconia* (*Advances in Ceramics* vol 3) eds A H Heuer and L W Hobbs (Columbus, OH: The American Ceramic Society Inc.) pp 1–24
[2] Lodermik W H, Milam D and Rainer F 1980 *Thin Solid Films* **73** 155
[3] Aleksandrov V I *et al* 1989 *Opt. Spectrosc.* **66** 548
[4] Blasse G and Grabmaier B C 1994 *Luminescent Materials* (Berlin: Springer) pp 27–28, 40–50
[5] Harrison H D E, McLamed N T and Subbaro E C 1963 *J. Electrochem. Soc.* **110** 23
[6] French R H, Glass S J, Ohuchi F S, Xu Y N, and Ching W Y 1994 *Phys. Rev. B Condens. Matter. third series* **49** 5133
[7] Ramos-Brito F, García-Hipólito M, Martínez-Martínez R, Martínez-Sánchez E and Falcony C 2004 *J. Phys. D: Appl. Phys.* **37** L13
[8] De la Rosa-Cruz E, Diaz-Torres L A, Salas P, Rodríguez R A, Kumar G A, Meneses M A, Mosiño J F, Hernández J M and Barbosa-García O 2003 *J. Appl. Phys.* **94** 3509
[9] Pereyra-Perea E, Estrada M R and García M 1998 *J. Phys.* D **31** L7
[10] Millers D, Grigorjeva L, Opalinska A and Lojkowski W 2003 *Solid State Phennom.* **94** 135
[11] Friend C S, Patra A, Kapoor R and Prasad P N 2002 *J. Phys. Chem.* B **106** 1909
[12] Reisfeld R, Zelner M and Patra A 2000 *J. Alloys Compd.* **147** 300
[13] Hase T, Kano T, Nakasawa E and Yamamoto H, 1990 Phosphor materials for cathode-ray tubes *Advances in Electronics and Electron Physics* vol 79, ed P W Hawkes (New York: Academic) p 271
[14] Phillippi C M and Mazdiyasni K S 1971 *J. Am. Ceram. Soc.* **54** 254
[15] Maczka M, Lutz E T G, Verbeek H J, Oskam K, Meijering A, Hanuza J, Stuivinga M 1999 *J. Phys. Chem. Solids* **60** 1909
[16] Asher I M, Papanicolau B and Anastassakis E 1976 *J. Phys. Chem. Solids* **37** 221
[17] Dexpert-Ghys J, Faucher M and Caro P 1984 *J. Solid State Chem.***54** 179
[18] Savoini B, Muñoz Santiuste J E, González R and Chen Y 1997 *J. Lumin.* **72** 715